Measurement of the W Boson Mass Using Electrons at Large Rapidities

B. Abbott,[46] M. Abolins,[43] V. Abramov,[19] B. S. Acharya,[12] I. Adam,[45] D. L. Adams,[53] M. Adams,[29] S. Ahn,[28] V. Akimov,[17] G. A. Alves,[2] N. Amos,[42] E. W. Anderson,[35] M. M. Baarmand,[48] V. V. Babintsev,[19] L. Babukhadia,[21] A. Baden,[39] B. Baldin,[28] S. Banerjee,[12] J. Bantly,[52] E. Barberis,[22] P. Baringer,[36] J. F. Bartlett,[28] A. Belyaev,[18] S. B. Beri,[10] I. Bertram,[20] V. A. Bezzubov,[19] P. C. Bhat,[28] V. Bhatnagar,[10] M. Bhattacharjee,[48] G. Blazey,[30] S. Blessing,[26] A. Boehnlein,[28] N. I. Bojko,[19] F. Borcherding,[28] A. Brandt,[53] R. Breedon,[23] G. Briskin,[52] R. Brock,[43] A. Bross,[28] D. Buchholz,[31] V. S. Burtovoi,[19] J. M. Butler,[40] W. Carvalho,[3] D. Casey,[43] Z. Casilum,[48] H. Castilla-Valdez,[15] D. Chakraborty,[48] K. M. Chan,[47] S. V. Chekulaev,[19] W. Chen,[48] D. K. Cho,[47] S. Choi,[14] S. Chopra,[26] B. C. Choudhary,[25] J. H. Christenson,[28] M. Chung,[29] D. Claes,[44] A. R. Clark,[22] W. G. Cobau,[39] J. Cochran,[25] L. Coney,[33] B. Connolly,[26] W. E. Cooper,[28] D. Coppage,[36] D. Cullen-Vidal,[52] M. A. C. Cummings,[30] D. Cutts,[52] O. I. Dahl,[22] K. Davis,[21] K. De,[53] K. Del Signore,[42] M. Demarteau,[28] D. Denisov,[28] S. P. Denisov,[19] H. T. Diehl,[28] M. Diesburg,[28] G. Di Loreto,[43] P. Draper,[53] Y. Ducros,[9] L. V. Dudko,[18] S. R. Dugad,[12] A. Dyshkant,[19] D. Edmunds,[43] J. Ellison,[25] V. D. Elvira,[48] R. Engelmann,[48] S. Eno,[39] G. Eppley,[55] P. Ermolov,[18] O. V. Eroshin,[19] J. Estrada,[47] H. Evans,[45] V. N. Evdokimov,[19] T. Fahland,[24] M. K. Fatyga,[47] S. Feher,[28] D. Fein,[21] T. Ferbel,[47] H. E. Fisk,[28] Y. Fisyak,[49] E. Flattum,[28] M. Fortner,[30] K. C. Frame,[43] S. Fuess,[28] E. Gallas,[28] A. N. Galyaev,[19] P. Gartung,[25] V. Gavrilov,[17] R. J. Genik II,[43] K. Genser,[28] C. E. Gerber,[28] Y. Gershtein,[52] B. Gibbard,[49] R. Gilmartin,[26] G. Ginther,[47] B. Gobbi,[31] B. Gómez,[5] G. Gómez,[39] P. I. Goncharov,[19] J. L. González Solís,[15] H. Gordon,[49] L. T. Goss,[54] K. Gounder,[25] A. Goussiou,[48] N. Graf,[49] P. D. Grannis,[48] D. R. Green,[28] J. A. Green,[35] H. Greenlee,[28] S. Grinstein,[1] P. Grudberg,[22] S. Grünendahl,[28] G. Guglielmo,[51] J. A. Guida,[21] J. M. Guida,[52] A. Gupta,[12] S. N. Gurzhiev,[19] G. Gutierrez,[28] P. Gutierrez,[51] N. J. Hadley,[39] H. Haggerty,[28] S. Hagopian,[26] V. Hagopian,[26] K. S. Hahn,[47] R. E. Hall,[24] P. Hanlet,[41] S. Hansen,[28] J. M. Hauptman,[35] C. Hays,[45] C. Hebert,[36] D. Hedin,[30] A. P. Heinson,[25] U. Heintz,[40] R. Hernández-Montoya,[15] T. Heuring,[26] R. Hirosky,[29] J. D. Hobbs,[48] B. Hoeneisen,[6] J. S. Hoftun,[52] F. Hsieh,[42] A. S. Ito,[28] S. A. Jerger,[43] R. Jesik,[32] T. Joffe-Minor,[31] K. Johns,[21] M. Johnson,[28] A. Jonckheere,[28] M. Jones,[27] H. Jöstlein,[28] S. Y. Jun,[31] S. Kahn,[49] E. Kajfasz,[8] D. Karmanov,[18] D. Karmgard,[26] R. Kehoe,[33] S. K. Kim,[14] B. Klima,[28] C. Klopfenstein,[23] B. Knuteson,[22] W. Ko,[23] J. M. Kohli,[10] D. Koltick,[34] A. V. Kostritskiy,[19] J. Kotcher,[49] A. V. Kotwal,[45] A. V. Kozelov,[19] E. A. Kozlovsky,[19] J. Krane,[35] M. R. Krishnaswamy,[12] S. Krzywdzinski,[28] M. Kubantsev,[37] S. Kuleshov,[17] Y. Kulik,[48] S. Kunori,[39] F. Landry,[43] G. Landsberg,[52] A. Leflat,[18] J. Li,[53] Q. Z. Li,[28] J. G. R. Lima,[3] D. Lincoln,[28] S. L. Linn,[26] J. Linnemann,[43] R. Lipton,[28] J. G. Lu,[4] A. Lucotte,[48] L. Lueking,[28] A. K. A. Maciel,[30] R. J. Madaras,[22] L. Magaña-Mendoza,[15] V. Manankov,[18] S. Mani,[23] H. S. Mao,[4] R. Markeloff,[30] T. Marshall,[32] M. I. Martin,[28] R. D. Martin,[29] K. M. Mauritz,[35] B. May,[31] A. A. Mayorov,[32] R. McCarthy,[48] J. McDonald,[26] T. McKibben,[29] J. McKinley,[43] T. McMahon,[50] H. L. Melanson,[28] M. Merkin,[18] K. W. Merritt,[28] C. Miao,[52] H. Miettinen,[55] A. Mincer,[46] C. S. Mishra,[28] N. Mokhov,[28] N. K. Mondal,[12] H. E. Montgomery,[28] M. Mostafa,[1] H. da Motta,[2] F. Nang,[21] M. Narain,[40] V. S. Narasimham,[12] H. A. Neal,[42] J. P. Negret,[5] D. Norman,[54] L. Oesch,[42] V. Oguri,[3] N. Oshima,[28] D. Owen,[43] P. Padley,[55] A. Para,[28] N. Parashar,[41] Y. M. Park,[13] R. Partridge,[52] N. Parua,[7] M. Paterno,[47] A. Patwa,[48] B. Pawlik,[16] J. Perkins,[53] M. Peters,[27] R. Piegaia,[1] H. Piekarz,[26] Y. Pischalnikov,[34] B. G. Pope,[43] H. B. Prosper,[26] S. Protopopescu,[49] J. Qian,[42] P. Z. Quintas,[28] S. Rajagopalan,[49] O. Ramirez,[29] N. W. Reay,[37] S. Reucroft,[41] M. Rijssenbeek,[48] T. Rockwell,[43] M. Roco,[28] P. Rubinov,[31] R. Ruchti,[33] J. Rutherfoord,[21] A. Sánchez-Hernández,[15] A. Santoro,[2] L. Sawyer,[38] R. D. Schamberger,[48] H. Schellman,[31] J. Sculli,[46] E. Shabalina,[18] C. Shaffer,[26] H. C. Shankar,[12] R. K. Shivpuri,[11] D. Shpakov,[48] M. Shupe,[21] R. A. Sidwell,[37] H. Singh,[25] J. B. Singh,[10] V. Sirotenko,[30] P. Slattery,[47] E. Smith,[51] R. P. Smith,[28] R. Snihur,[31] G. R. Snow,[44] J. Snow,[50] S. Snyder,[49] J. Solomon,[29] X. F. Song,[4] M. Sosebee,[53] N. Sotnikova,[18] M. Souza,[2] N. R. Stanton,[37] G. Steinbrück,[51] R. W. Stephens,[53] M. L. Stevenson,[22] F. Stichelbaut,[49] D. Stoker,[24] V. Stolin,[17] D. A. Stoyanova,[19] M. Strauss,[51] K. Streets,[46] M. Strovink,[22] L. Stutte,[28] A. Sznajder,[3] P. Tamburello,[39] J. Tarazi,[24] M. Tartaglia,[28] T. L. T. Thomas,[31] J. Thompson,[39] D. Toback,[39] T. G. Trippe,[22] A. S. Turcot,[42] P. M. Tuts,[45] P. van Gemmeren,[28] V. Vaniev,[19] N. Varelas,[29] A. A. Volkov,[19] A. P. Vorobiev,[19] H. D. Wahl,[26] J. Warchol,[33] G. Watts,[56] M. Wayne,[33] H. Weerts,[43] A. White,[53] J. T. White,[54] J. A. Wightman,[35] S. Willis,[30] S. J. Wimpenny,[25] J. V. D. Wirjawan,[54] J. Womersley,[28] D. R. Wood,[41] R. Yamada,[28] P. Yamin,[49] T. Yasuda,[28] K. Yip,[28] S. Youssef,[26] J. Yu,[28] Y. Yu,[14] M. Zanabria,[5] Z. Zhou,[35] Z. H. Zhu,[47] M. Zielinski,[47] D. Zieminska,[32] A. Zieminski,[32] V. Zutshi,[47] E. G. Zverev,[18] and A. Zylberstejn[9]

 0031-9007/00/84(2)/222(6)$15.00

(D0 Collaboration)
[1]*Universidad de Buenos Aires, Buenos Aires, Argentina*
[2]*LAFEX, Centro Brasileiro de Pesquisas Físicas, Rio de Janeiro, Brazil*
[3]*Universidade do Estado do Rio de Janeiro, Rio de Janeiro, Brazil*
[4]*Institute of High Energy Physics, Beijing, People's Republic of China*
[5]*Universidad de los Andes, Bogotá, Colombia*
[6]*Universidad San Francisco de Quito, Quito, Ecuador*
[7]*Institut des Sciences Nucléaires, IN2P3-CNRS, Universite de Grenoble 1, Grenoble, France*
[8]*Centre de Physique des Particules de Marseille, IN2P3-CNRS, Marseille, France*
[9]*DAPNIA/Service de Physique des Particules, CEA, Saclay, France*
[10]*Panjab University, Chandigarh, India*
[11]*Delhi University, Delhi, India*
[12]*Tata Institute of Fundamental Research, Mumbai, India*
[13]*Kyungsung University, Pusan, Korea*
[14]*Seoul National University, Seoul, Korea*
[15]*CINVESTAV, Mexico City, Mexico*
[16]*Institute of Nuclear Physics, Kraków, Poland*
[17]*Institute for Theoretical and Experimental Physics, Moscow, Russia*
[18]*Moscow State University, Moscow, Russia*
[19]*Institute for High Energy Physics, Protvino, Russia*
[20]*Lancaster University, Lancaster, United Kingdom*
[21]*University of Arizona, Tucson, Arizona 85721*
[22]*Lawrence Berkeley National Laboratory and University of California, Berkeley, California 94720*
[23]*University of California, Davis, California 95616*
[24]*University of California, Irvine, California 92697*
[25]*University of California, Riverside, California 92521*
[26]*Florida State University, Tallahassee, Florida 32306*
[27]*University of Hawaii, Honolulu, Hawaii 96822*
[28]*Fermi National Accelerator Laboratory, Batavia, Illinois 60510*
[29]*University of Illinois at Chicago, Chicago, Illinois 60607*
[30]*Northern Illinois University, DeKalb, Illinois 60115*
[31]*Northwestern University, Evanston, Illinois 60208*
[32]*Indiana University, Bloomington, Indiana 47405*
[33]*University of Notre Dame, Notre Dame, Indiana 46556*
[34]*Purdue University, West Lafayette, Indiana 47907*
[35]*Iowa State University, Ames, Iowa 50011*
[36]*University of Kansas, Lawrence, Kansas 66045*
[37]*Kansas State University, Manhattan, Kansas 66506*
[38]*Louisiana Tech University, Ruston, Louisiana 71272*
[39]*University of Maryland, College Park, Maryland 20742*
[40]*Boston University, Boston, Massachusetts 02215*
[41]*Northeastern University, Boston, Massachusetts 02115*
[42]*University of Michigan, Ann Arbor, Michigan 48109*
[43]*Michigan State University, East Lansing, Michigan 48824*
[44]*University of Nebraska, Lincoln, Nebraska 68588*
[45]*Columbia University, New York, New York 10027*
[46]*New York University, New York, New York 10003*
[47]*University of Rochester, Rochester, New York 14627*
[48]*State University of New York, Stony Brook, New York 11794*
[49]*Brookhaven National Laboratory, Upton, New York 11973*
[50]*Langston University, Langston, Oklahoma 73050*
[51]*University of Oklahoma, Norman, Oklahoma 73019*
[52]*Brown University, Providence, Rhode Island 02912*
[53]*University of Texas, Arlington, Texas 76019*
[54]*Texas A&M University, College Station, Texas 77843*
[55]*Rice University, Houston, Texas 77005*
[56]*University of Washington, Seattle, Washington 98195*
(Received 17 September 1999)

We report a measurement of the W boson mass based on an integrated luminosity of 82 pb^{-1} from $p\overline{p}$ collisions at $\sqrt{s} = 1.8$ TeV recorded in 1994–1995 by the D0 detector at the Fermilab Tevatron.

We identify W bosons by their decays to $e\nu$, where the electron is detected in the forward calorimeters. We extract the mass by fitting the transverse mass and the electron and neutrino transverse momentum spectra of 11 089 W boson candidates. We measure $M_W = 80.691 \pm 0.227$ GeV. By combining this measurement with our previously published central calorimeter results from data taken in 1992–1993 and 1994–1995, we obtain $M_W = 80.482 \pm 0.091$ GeV.

PACS numbers: 14.70.Fm, 12.15.Ji, 13.38.Be, 13.85.Qk

In the standard model (SM) of the electroweak interactions, the mass of the W boson is predicted to be

$$M_W = \left(\frac{\pi\alpha(M_Z^2)}{\sqrt{2}G_F}\right)^{\frac{1}{2}} \frac{1}{\sin\theta_W\sqrt{1-\Delta r}}. \tag{1}$$

In the "on-shell" scheme [1] $\cos\theta_W = M_W/M_Z$, where M_Z is the Z boson mass. A measurement of M_W, together with M_Z [2], the Fermi constant (G_F), and the electromagnetic coupling constant (α), experimentally determines the weak radiative corrections Δr. Compared to the formulation in [1] where α was defined at $Q^2 = 0$, we have absorbed purely electromagnetic corrections into the value of α by evaluating it at $Q^2 = M_Z^2$. The dominant SM contributions to Δr arise from loop diagrams involving the top quark and the Higgs boson. If additional particles coupling to the W boson exist, they also give contributions to Δr. Therefore, a measurement of M_W is a stringent experimental test of SM predictions. Within the SM, measurements of M_W and the mass of the top quark constrain the mass of the Higgs boson.

We report a new measurement of the W boson mass using electrons detected at forward angles. We use 82 pb^{-1} of data recorded with the D0 detector during the 1994–1995 run of the Fermilab Tevatron $p\overline{p}$ collider. This forward electron measurement, in addition to increasing the statistical precision, complements our previous measurement with central electrons [3] because the more complete combined rapidity coverage gives useful constraints on model parameters that reduce the systematic error. A more complete account of this measurement can be found in Ref. [4].

At the Tevatron, W bosons are produced through $q\overline{q}'$ annihilation. $W \to e\nu$ decays are characterized by an electron with large transverse energy (E_T) and significant transverse momentum imbalance ($\not{p}_T$) due to the undetected neutrino. The particles recoiling against the W boson are referred to collectively as the "underlying event."

The D0 detector [5] consists of three major subsystems: a tracking detector, a calorimeter, and a muon spectrometer. The tracking detector consists of a vertex drift chamber, a central drift chamber (CDC), and two forward drift chambers (FDC). The CDC covers the pseudorapidity [$\eta = -\ln(\tan\frac{\theta}{2})$ where θ is the polar angle] region $|\eta| < 1.0$. The FDC extend the coverage to $|\eta| < 3.0$. The central calorimeter (CC) and two end calorimeters (EC) provide almost uniform coverage for particles with $|\eta| < 4$.

At the trigger level, we require $\not{p}_T > 15$ GeV and an energy cluster in the electromagnetic (EM) calorimeter with $E_T > 20$ GeV. The cluster must be isolated and have a shape consistent with that of an electron shower.

During event reconstruction, electrons are identified as energy clusters in the EM calorimeter, which satisfy isolation and shower shape cuts and have a drift chamber track pointing to the cluster centroid. We determine forward electron energies by adding the energy depositions in the calorimeter within a cone of radius 20 cm, centered on the cluster centroid. The electron momentum [$\vec{p}(e)$] is determined by combining its energy with the direction obtained from the shower centroid position and the drift chamber track. The trajectory of the electron defines the position of the event vertex along the beam line.

We measure the sum of the transverse momenta of all particles recoiling against the W boson, $\vec{u}_T = \sum_i E_i \sin\theta_i \hat{u}_i^T$, where E_i is the energy deposition in calorimeter cell i, $\hat{u}_i^T$ is the unit transverse vector pointing from the beam line to the cell center, and θ_i is the polar angle defined by the cell center and the event vertex. The $\vec{u}_T$ calculation excludes cells occupied by the electron. The transverse momenta of the neutrino, $\vec{p}_T(\nu) = -\vec{p}_T(e) - \vec{u}_T$, and the W boson, $\vec{p}_T(W) = -\vec{u}_T$, are inferred from momentum conservation.

We select a W boson sample of 11 089 events by requiring $p_T(\nu) > 30$ GeV, $u_T < 15$ GeV, and an electron candidate with $1.5 < |\eta| < 2.5$ and $p_T(e) > 30$ GeV.

We extract the W boson mass from the spectra of the electron $p_T(e)$, neutrino $p_T(\nu)$, and the transverse mass, $m_T = \sqrt{2p_T(e)p_T(\nu)(1-\cos\Delta\phi)}$, where $\Delta\phi$ is the azimuthal separation between the two leptons. For each spectrum we perform a maximum likelihood fit to the data using probability density functions from a Monte Carlo program. We model the production dynamics of W bosons and the detector response to predict the spectra. The m_T, $p_T(e)$, and $p_T(\nu)$ spectra have quite different sensitivities to the W boson production dynamics and the recoil momentum measurement. By performing the measurement using all three spectra we provide a powerful cross-check with complementary systematics.

Z bosons decaying to electrons provide an important control sample. We use them to calibrate the detector response to the underlying event and electrons and to constrain the model for vector boson production used in the Monte Carlo simulations. We trigger on $Z \to ee$ events having at least two EM clusters with $E_T > 20$ GeV. We accept $Z \to ee$ decays with at least one forward electron with $1.5 < |\eta| < 2.5$ and another forward or central

($|\eta| < 1.0$) electron. A central electron is required to have $p_T > 25$ GeV but is allowed not to have a matching drift chamber track. The forward electron candidate is required to have $p_T > 30$ GeV and a matching drift chamber track. This selection accepts 1687 Z boson events.

We use a fast Monte Carlo program developed for the central electron analyses [3,6], with modifications in the simulation of forward electron events. The program generates W and Z bosons with the η and p_T spectra given by a calculation [7] which used soft gluon resummation and the MRST [8] parton distribution functions. We use the relativistic Breit-Wigner line shape with mass-dependent width, skewed by the mass dependence of the parton luminosity. The measured W and Z boson intrinsic widths [9] are used. The angular distribution of the decay electrons includes a $p_T(W)$-dependent $\mathcal{O}(\alpha_s^2)$ correction [10]. The program also generates $W \to e\nu\gamma$ [11], $Z \to ee\gamma$ [11], and $W \to \tau\nu \to e\nu\overline{\nu}\nu$ decays.

The program smears the generated $\vec{p}(e)$ and $\vec{u}_T$ vectors using a parametrized detector response model and applies inefficiencies introduced by the trigger and off-line selection requirements. Backgrounds are added to the Monte Carlo samples. The parameters are adjusted to match the data.

The electron energy resolution ($\delta E/E$) is parametrized by calorimeter sampling, noise, and constant terms. In the Monte Carlo simulation of forward electrons we use a sampling term of $15.7\%/\sqrt{E/\mathrm{GeV}}$, derived from beam tests [12]. The noise term is determined by pedestal distributions taken from the W boson data. We constrain the constant term to $c_{\mathrm{EC}} = 1.0^{+0.6}_{-1.0}\%$ by requiring that the predicted width of the dielectron invariant mass spectrum be consistent with the Z boson data.

Beam tests show that the electron energy response of the end calorimeter can be parametrized by a scale factor α_{EC} and an offset δ_{EC}. We determine these *in situ* using $Z \to ee$ decays [4]. For forward electrons we obtain $\delta_{\mathrm{EC}} = -0.1 \pm 0.7$ GeV and $\alpha_{\mathrm{EC}} = 0.951\,79 \pm 0.001\,87$ by fitting the observed mass spectra while constraining the resonance masses to the Z boson mass. The uncertainty on α_{EC} is dominated by the finite size of the Z boson sample. Figure 1 shows the observed mass spectra from the dielectron samples and the line shapes predicted by the Monte Carlo simulation for the fitted values of c_{EC}, α_{EC}, and δ_{EC}. The background was determined from a sample of events with two EM clusters failing electron quality cuts. The calibration of the electron polar angle [4] uses muons from $p\overline{p}$ collisions and cosmic rays to calibrate the drift chambers, and $Z \to ee$ decays to align the EC with the drift chambers.

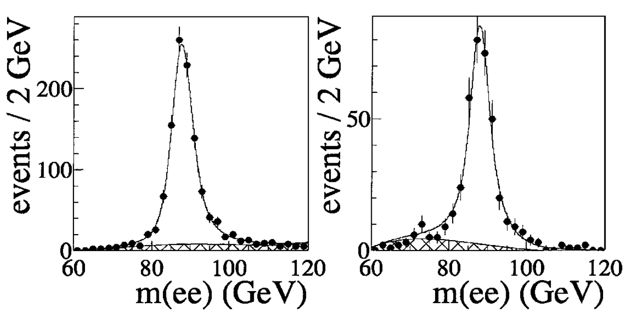

FIG. 1. The dielectron invariant mass distribution of the CC/EC (left, χ^2/d.o.f. = 14/19) and EC/EC (right, χ^2/d.o.f. = 12/17) Z boson data (•). The solid line shows the fitted signal plus background shape and the small hatched area shows the background. The fitting window is $70 < m(ee) < 110$ GeV.

We calibrate the response of the detector to the underlying event using the Z boson data sample. In $Z \to ee$ events, momentum conservation requires $\vec{p}_T(ee) = -\vec{u}_T$, where $\vec{p}_T(ee)$ is the sum of the two electron p_T vectors [4]. We constrain the detector response R_{rec} using the mean value of the $\vec{p}_T(ee) + \vec{u}_T$ projection on the inner bisector of the two electron directions. Z boson events with two forward electrons give a recoil response measurement that is consistent with the measurement performed in the central dielectron analysis[3].

The recoil momentum resolution has two components: a stochastic term, which we model as $s_{\mathrm{rec}}/\sqrt{p_T/\mathrm{GeV}}$; and the detector noise and pile-up, which we model using the scaled $\not{p}_T$ from random $p\overline{p}$ interactions [4]. We constrain the model by comparing the observed rms of $\vec{p}_T(ee) + \vec{u}_T/R_{\mathrm{rec}}$ with Monte Carlo predictions. The model tuned for the central electron analysis [3] gives a good description of the $\vec{p}_T(ee) + \vec{u}_T/R_{\mathrm{rec}}$ distributions for our Z boson event sample. Figure 2 shows the comparison between the W boson Monte Carlo and the data of the projection of recoil momentum on the direction of the forward electron ($u_\parallel$) and on a direction perpendicular to the electron momentum ($u_\perp$).

Backgrounds in the W boson sample are due to $W \to \tau\nu \to e\nu\overline{\nu}\nu$ decays (1%, included in the Monte Carlo simulation), hadrons misidentified as electrons ($3.64 \pm 0.78\%$, determined from the data), and $Z \to ee$ decays ($0.26 \pm 0.02\%$, determined from HERWIG [13] and GEANT [14] simulations). Their shapes are included in the probability density functions used in the fits. The results of the fits to the m_T, $p_T(e)$, and $p_T(\nu)$ distributions are shown in Fig. 3 and Table I.

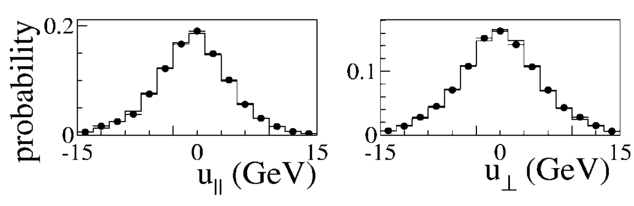

FIG. 2. Probability distributions of $u_\parallel$ (left, χ^2/d.o.f. = 25/15) and $u_\perp$ (right, χ^2/d.o.f. = 14/15) for the forward W boson data (•) and the Monte Carlo simulation (—).

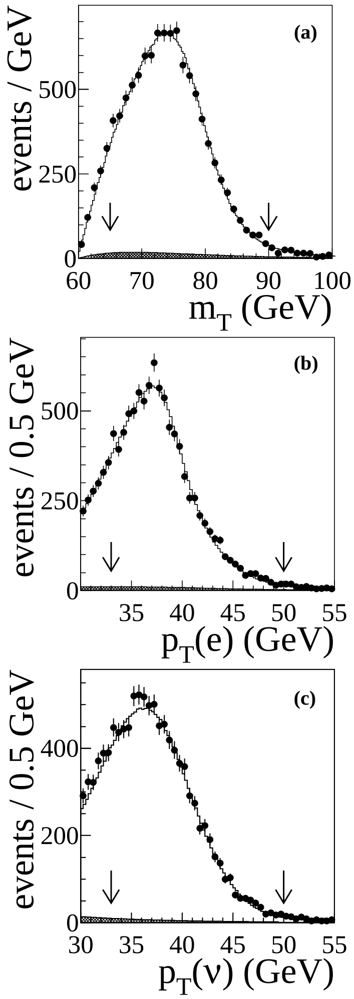

FIG. 3. Spectra of (a) m_T, (b) $p_T(e)$, and (c) $p_T(\nu)$ from the data (•), the fit (—), and the backgrounds (shaded). The arrows indicate the fit windows.

We estimate the systematic uncertainties in M_W (Table II) by varying the Monte Carlo parameters withintheir uncertainties. We assign an uncertainty that characterizes the range of variations in M_W obtained when employing several recent parton distribution functions: MRST, MRS(A′) [15], MRSR2 [16], CTEQ3M [17], CTEQ4M [18], and CTEQ5M [19]. We have checked that the pdf's reproduce the $\eta(e)$ distribution for the W bosons well [4]. We allow the $p_T(W)$ spectrum to vary within constraints derived from the $p_T(ee)$ spectrum of the Z boson data [3] and from Λ_{QCD} [3]. Smaller uncertainties in M_W are due to the removal of the cells occupied by the electron from the computation of $\vec{u}_T$, and the modeling of trigger and selection biases [4]. The uncertainty due to radiative decays contains an estimate of the effect of neglecting double photon emission in the Monte Carlo simulation [20].

The total systematic errors are shown in Table I. The good agreement of the three fits shows that our simulation models the W boson production dynamics and the detector response well. Fits to the data in bins of luminosity, $\phi(e)$, $\eta(e)$, and u_T and with changes to the fit window show no evidence of systematic biases.

TABLE I. The fitted values and errors of the forward W boson mass measurements in GeV. The confidence level (C.L.) is given by the χ^2 probability of the fit.

Fit	Mass	Stat.	Syst.	Total error	C.L.
m_T fit	80.757	0.107	0.204	0.230	81%
$p_T(e)$ fit	80.547	0.128	0.203	0.240	8%
$p_T(\nu)$ fit	80.740	0.159	0.310	0.348	33%

As a consistency check, we fit the transverse mass distribution of the $Z \rightarrow ee$ events. We retain one electron in the EC and ignore the energy of the other electron (in the CC or EC). The fitted Z boson mass (Fig. 4) is 92.004 ± 0.895 (stat) GeV for the CC/EC sample, and 91.074 ± 0.299 (stat) GeV for the EC/EC sample. The combined mass is 91.167 ± 0.284 (stat) GeV. These results are consistent with the input Z boson mass we used to calibrate the detector response.

We combine the m_T, $p_T(e)$, and $p_T(\nu)$ measurements of M_W using a full covariance matrix that takes into account correlations between all the parameters describing the W boson production model and detector response, as well as the statistical correlations. The combination of all three forward electron measurements yields a W boson mass of $M_W = 80.691 \pm 0.227$ GeV. We also combine the three central electron measurements [3] with the three forward W boson mass measurements to obtain the combined 1994–1995 data measurement of $M_W = 80.498 \pm 0.095$ GeV. The χ^2 is 5.1/5 d.o.f., with a probability of 41%. Further combining this with the measurement from

TABLE II. Uncertainties in the combined m_T, $p_T(e)$, and $p_T(\nu)$ W boson mass measurement in MeV, for the forward sample (first column), and the combined central and forward 1994–1995 sample (second column).

Source	Forward	Forward + Central
W boson statistics	108	61
Z boson statistics	181	59
Calorimeter linearity	52	25
Calorimeter uniformity	⋯	8
Electron resolution	42	19
Electron angle calibration	20	10
Recoil response	17	25
Recoil resolution	42	25
Electron removal	4	12
Trigger and selection bias	5	3
Backgrounds	20	9
Parton distribution functions	17	7
Parton luminosity	2	4
$p_T(W)$ spectrum	25	15
W boson width	10	10
Radiative decays	1	12

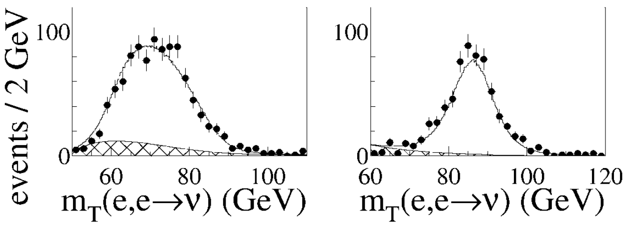

FIG. 4. Spectra of the Z boson transverse mass from the CC/EC data (left) and the EC/EC data (right). The superimposed curves show the maximum likelihood fits and the hatched regions show the estimated backgrounds.

the 1992–1993 [6] data gives the 1992–1995 data measurement of $M_W = 80.482 \pm 0.091$ GeV. This measurement subsumes all previously published measurements of the W boson mass by D0.

From Eq. (1), using $\alpha(M_Z^2) = (128.88 \pm 0.09)^{-1}$ [21] we find $\Delta r = -0.0322 \pm 0.0059$, which establishes the existence of loop corrections to M_W at the level of 5 standard deviations. Taken together with our measured top quark mass ($m_t = 172.1 \pm 7.1$ GeV [22]), our value of the W boson mass is consistent with measurements by CDF [23] and the LEP experiments [2] and with the SM prediction for a low mass Higgs boson (i.e., $m_H <$ 100 GeV), and is in even better agreement with predictions [24] in the MSSM framework.

We thank the Fermilab and collaborating institution staffs for contributions to this work and acknowledge support from the Department of Energy and National Science Foundation (U.S.A.), Commissariat á L'Energie Atomique (France), Ministry for Science and Technology and Ministry for Atomic Energy (Russia), CAPES and CNPq (Brazil), Departments of Atomic Energy and Science and Education (India), Colciencias (Colombia), CONACyT (Mexico), Ministry of Education and KOSEF (Korea), and CONICET and UBACyT (Argentina).

[1] A. Sirlin, Phys. Rev. D **22**, 971 (1980); W. Marciano and A. Sirlin, Phys. Rev. D **22**, 2695 (1980); **31**, 213(E) (1985).
[2] The LEP Collaborations, the LEP Electroweak Working Group, and the SLD Heavy Flavour and Electroweak Groups, CERN Report No. CERN-EP/99-15 (unpublished).
[3] D0 Collaboration, B. Abbott *et al.*, Phys. Rev. D **58**, 092003 (1998); D0 Collaboration, B. Abbott *et al.*, Phys. Rev. Lett. **80**, 3008 (1998).
[4] D0 Collaboration, B. Abbott *et al.*, hep-ex/9908057, and references therein.
[5] D0 Collaboration, S. Abachi *et al.*, Nucl. Instrum. Methods Phys. Res., Sect. A **338**, 185 (1994).
[6] D0 Collaboration, S. Abachi *et al.*, Phys. Rev. Lett. **77**, 3309 (1996); D0 Collaboration, B. Abbott *et al.*, Phys. Rev. D **58**, 012002 (1998).
[7] G. A. Ladinsky and C.-P. Yuan, Phys. Rev. D **50**, 4239 (1994).
[8] A. D. Martin, R. G. Roberts, W. J. Stirling, and R. S. Thorne, Eur. Phys. J. C **4**, 463 (1998).
[9] D0 Collaboration, S. Abachi *et al.*, Phys. Rev. Lett. **75**, 1456 (1995).
[10] E. Mirkes, Nucl. Phys. **B387**, 3 (1992).
[11] F. A. Berends and R. Kleiss, Z. Phys. C **27**, 365 (1985).
[12] H. Aihara *et al.*, Nucl. Instrum. Methods Phys. Res., Sect. A **325**, 393 (1993).
[13] G. Marchesini *et al.*, Comput. Phys. Commun. **67**, 465 (1992), release 5.7.
[14] F. Carminati *et al.*, GEANT Users Guide, CERN Program Library W5013, 1991 (unpublished).
[15] A. D. Martin, W. J. Stirling, and R. G. Roberts, Phys. Rev. D **50**, 6734 (1994); **51**, 4756 (1995).
[16] A. D. Martin, R. G. Roberts, and W. J. Stirling, Phys. Lett. B **387**, 419 (1996).
[17] H. L. Lai *et al.*, Phys. Rev. D **51**, 4763 (1995).
[18] H. L. Lai *et al.*, Phys. Rev. D **55**, 1280 (1997).
[19] H. L. Lai *et al.*, hep-ph/9903282 (unpublished).
[20] U. Baur *et al.*, Phys. Rev. D **56**, 140 (1997), and references therein.
[21] C. Caso *et al.*, Eur. Phys. J. C **3**, 1 (1998).
[22] D0 Collaboration, B. Abbott *et al.*, Phys. Rev. Lett. **80**, 2063 (1998); D0 Collaboration, B. Abbott *et al.*, Phys. Rev. D **60**, 052001 (1999).
[23] CDF Collaboration and D0 Collaboration, F. Abe *et al.*, and B. Abbott *et al.*, Fermilab Report No. Fermilab-conf-99-173-e, in Proceedings of the 34th Rencontres de Moriond: Electroweak Interactions and Unified Theories, Les Arcs, France, 1999 (to be published).
[24] D. Pierce *et al.*, Nucl. Phys. **B491**, 3 (1997), and references therein.